Supporting Information for: Porosity-Permeability Relationships in Mudstone from Pore-Scale Fluid Flow Simulations using the Lattice Boltzmann Method

Harsh Biren Vora[1], Brandon Dugan[2]

[1]Department of Earth, Environment and Planetary Sciences, Rice University, Houston, TX 77005

[2]Department of Geophysics, Colorado School of Mines, Golden, CO 80401

Contents of this File:

Figures S1 and S2

Tables S1 to S4

Introduction:

This supporting information includes six parts:

(1) Incorporating heterogenous platelet geometry in mudstone models [Fig. S1]

(2) Compaction data from smectite, kaolinite and intermediate mudstone models [Table S1]

(3) Compaction data from natural mudstone models, *NM1* and *NM2* [Table S2]

(4) Evolution of vertical tortuosity (τ_v) during compaction and fluid injection [Fig. S2]

(5) Microfracture growth data in compacted intermediate mudstone model [Table S3]

(6) Macrofracture propagation data in compacted intermediate mudstone model [Table S4]

Figure S1: Scaled-down model of mudstone pore structure *NM2* (ϕ=0.79), designed after sample 1324B-7H-7. The *NM2* mudstone model consists of 31% smectite, 41% illite and 28% chlorite by volume. (a) Cross sectional view of *NM2* pore structure with bedding layers consisting of smectite, illite and chlorite platelets; (b) Orthogonal view of *NM2*; and (c) Cross sectional view of *NM2* pore structure with platelet rotation (θ=10°) and directions of vertical (q_v) and horizontal flow (q_h).

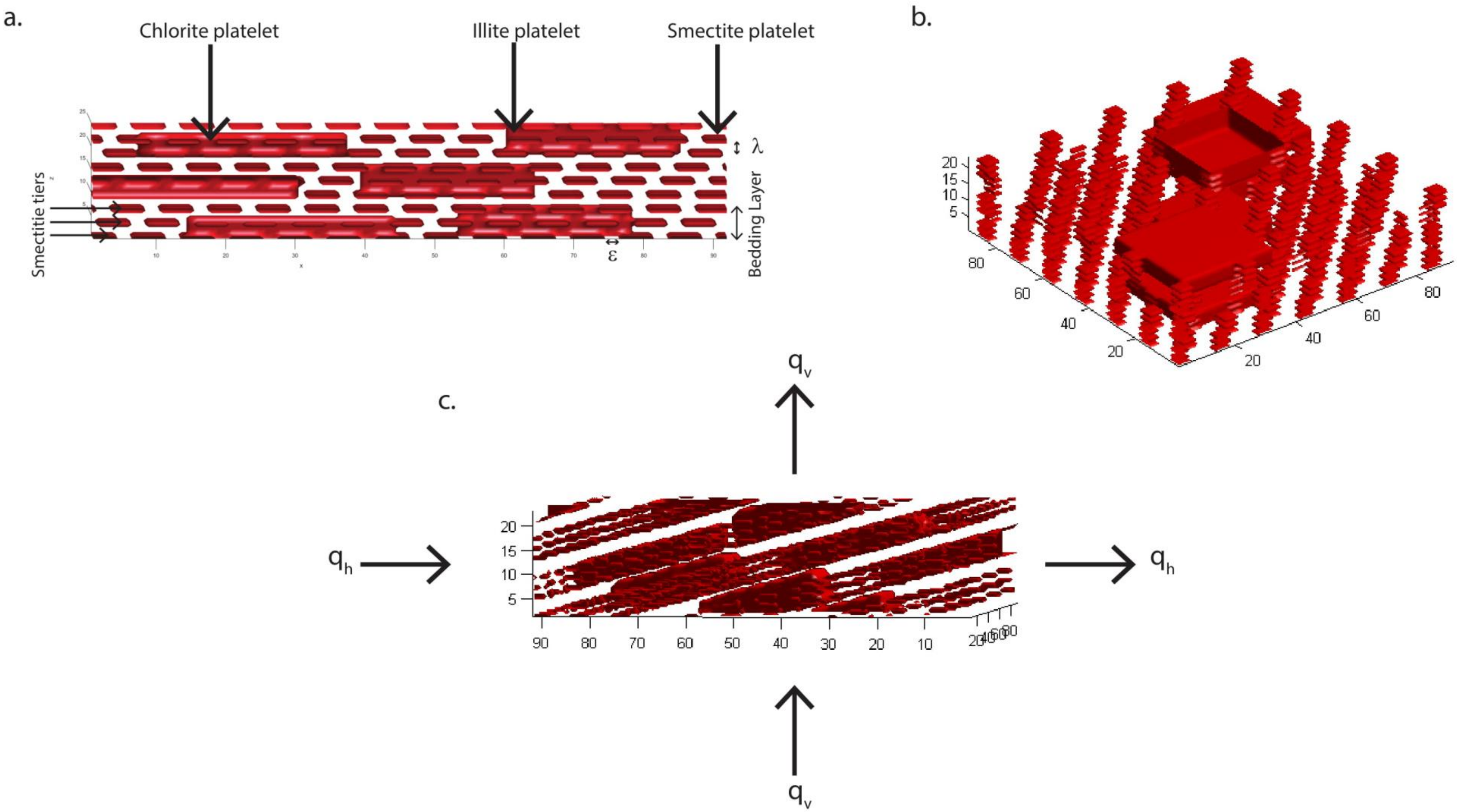

Table S1: Vertical (q_v) and horizontal (q_h) flux during compaction of kaolinite, smectite and intermediate mudstone models, simulated by step-wise decrease in intrabed (ξ), interbed pore throat diameters (λ) and orientation (θ).

Model	Step	Porosity \ ϕ	Intrabed Pore Throat Width ξ	Interbed Pore Throat Width λ	Platelet Orientation Θ	Vertical Flux q_v	Reynolds Number Vertical flow Re_v	Vertical Permeability k_v	Vertical Tortuosity τ_v	Horizontal Flux q_h	Reynolds Number Horizontal flow Re_h	Horizontal Permeability k_h	Horizontal Tortuosity τ_h
			(nm)	(nm)	Degrees	(m/s)		(m^2)		(m/s)		(m^2)	
Kaolinite	1	0.76	3.60×10^{2}	3.60×10^{2}	45	7.15×10^{-1}	2.41×10^{0}	8.31×10^{-15}	3.98	1.12×10^{-1}	1.88×10^{-2}	1.10×10^{-14}	3.98
Kaolinite	2	0.68	2.60×10^{2}	2.60×10^{2}	35	3.56×10^{-1}	1.20×10^{0}	3.42×10^{-15}	5.68	5.16×10^{-2}	8.69×10^{-3}	4.96×10^{-15}	4.36
Kaolinite	3	0.58	1.80×10^{2}	1.80×10^{2}	25	9.81×10^{-2}	3.31×10^{-1}	7.84×10^{-16}	8.15	1.77×10^{-2}	2.99×10^{-3}	1.68×10^{-15}	4.53
Kaolinite	4	0.46	1.20×10^{2}	1.20×10^{2}	20	2.63×10^{-2}	8.85×10^{-2}	1.78×10^{-16}	11.07	9.27×10^{-3}	1.56×10^{-3}	8.67×10^{-16}	4.97
Kaolinite	5	0.35	8.00×10^{1}	8.00×10^{1}	15	5.73×10^{-3}	1.93×10^{-2}	3.42×10^{-17}	14.30	2.33×10^{-3}	3.93×10^{-4}	2.16×10^{-16}	5.00
Kaolinite	6	0.28	6.00×10^{1}	6.00×10^{1}	10	1.92×10^{-3}	6.49×10^{-3}	1.07×10^{-17}	16.61	8.69×10^{-4}	1.47×10^{-4}	8.02×10^{-17}	4.29
Kaolinite	7	0.19	4.00×10^{1}	4.00×10^{1}	5	3.91×10^{-4}	1.32×10^{-3}	2.02×10^{-18}	19.80	2.60×10^{-4}	4.39×10^{-5}	2.39×10^{-17}	3.31
Kaolinite	8	0.14	4.00×10^{1}	4.00×10^{1}	0	1.23×10^{-4}	4.14×10^{-4}	6.33×10^{-19}	21.64	1.56×10^{-4}	2.63×10^{-5}	1.43×10^{-17}	1.74
Smectite	1	0.80	9.00×10^{0}	9.00×10^{0}	45	3.56×10^{-1}	4.00×10^{-2}	6.84×10^{-17}	7.08	4.18×10^{-2}	9.40×10^{-5}	1.33×10^{-16}	7.08
Smectite	2	0.76	7.00×10^{0}	7.00×10^{0}	35	2.10×10^{-1}	2.36×10^{-2}	3.61×10^{-17}	9.31	5.08×10^{-2}	1.14×10^{-4}	1.60×10^{-16}	6.88
Smectite	3	0.72	5.00×10^{0}	5.00×10^{0}	25	1.08×10^{-1}	1.21×10^{-2}	1.63×10^{-17}	12.03	4.11×10^{-2}	9.24×10^{-5}	1.29×10^{-16}	6.27
Smectite	4	0.66	4.00×10^{0}	4.00×10^{0}	15	3.50×10^{-2}	3.93×10^{-3}	4.60×10^{-18}	15.44	1.66×10^{-2}	3.72×10^{-5}	5.16×10^{-17}	5.06
Smectite	5	0.58	3.00×10^{0}	3.00×10^{0}	10	5.02×10^{-3}	5.64×10^{-4}	5.59×10^{-19}	20.10	3.18×10^{-3}	7.15×10^{-6}	9.85×10^{-18}	4.63
Smectite	6	0.45	2.00×10^{0}	2.00×10^{0}	5	3.04×10^{-4}	3.42×10^{-5}	2.77×10^{-20}	27.95	2.79×10^{-4}	6.28×10^{-7}	8.59×10^{-19}	3.74
Smectite	7	0.16	1.00×10^{0}	1.00×10^{0}	0	1.84×10^{-7}	2.06×10^{-8}	1.30×10^{-23}	50.65	3.06×10^{-7}	6.88×10^{-10}	9.35×10^{-22}	1.71
Intermediate	1	0.73	13.71×10^{1}	13.71×10^{1}	45	1.39×10^{-1}	3.12×10^{-1}	6.10×10^{-16}	6.72	1.75×10^{-2}	1.12×10^{-3}	1.11×10^{-15}	6.72
Intermediate	2	0.66	10.28×10^{1}	10.28×10^{1}	35	3.73×10^{-2}	8.37×10^{-2}	1.38×10^{-16}	9.60	7.07×10^{-3}	4.54×10^{-4}	4.44×10^{-16}	7.11
Intermediate	3	0.60	80.00×10^{0}	80.00×10^{0}	25	1.73×10^{-2}	3.88×10^{-2}	5.59×10^{-17}	12.79	5.78×10^{-3}	3.71×10^{-4}	3.60×10^{-16}	6.68
Intermediate	4	0.50	57.14×10^{0}	57.14×10^{0}	20	6.95×10^{-3}	1.56×10^{-2}	1.93×10^{-17}	16.88	3.00×10^{-3}	1.93×10^{-4}	1.86×10^{-16}	7.06
Intermediate	5	0.44	45.71×10^{0}	45.71×10^{0}	15	2.98×10^{-3}	6.70×10^{-3}	7.58×10^{-18}	20.03	1.45×10^{-3}	9.31×10^{-5}	8.93×10^{-17}	6.46
Intermediate	6	0.35	34.28×10^{0}	34.28×10^{0}	10	1.06×10^{-3}	2.38×10^{-3}	2.45×10^{-8}	24.45	7.22×10^{-4}	4.64×10^{-5}	4.43×10^{-17}	5.60
Intermediate	7	0.25	22.85×10^{0}	22.85×10^{0}	5	2.48×10^{-4}	5.57×10^{-4}	5.16×10^{-19}	30.30	2.33×10^{-4}	1.49×10^{-5}	1.42×10^{-17}	4.16
Intermediate	8	0.07	11.42×10^{0}	11.42×10^{0}	0	5.54×10^{-6}	1.24×10^{-5}	1.02×10^{-20}	41.61	7.68×10^{-6}	4.93×10^{-7}	4.68×10^{-19}	1.83

Table S2: Vertical (q_v) and horizontal (q_h) flux during compaction of *NM1* (designed after sample 1324C-1H-1) and *NM2* (designed after sample 1324B-7H-7) mudstone models, simulated by step-wise decrease in intrabed (ξ), interbed pore throat diameters (λ) and orientation (θ).

Model	**Step**	***Porosity*** ϕ	**Intrabed Pore Throat Width** ξ	**Interbed Pore Throat Width** λ	**Platelet Orientation** Θ	**Vertical Flux** q_v	**Reynolds Number Vertical flow** Re_v	**Vertical Permeability** k_v	**Vertical Tortuosity** τ_v	**Horizontal Flux** q_h	**Reynolds Number Horizontal flow** Re_h	**Horizontal Permeability** k_h	**Horizontal Tortuosity** τ_h
			(nm)	(nm)	Degrees	(m/s)		(m^2)		(m/s)		(m^2)	
NM1	1	0.72	5.05×10^{1}	5.05×10^{1}	15	5.03×10^{-2}	2.71×10^{-2}	1.54×10^{-16}	11.30	5.08×10^{-2}	7.42×10^{-4}	1.39×10^{-15}	3.91
NM1	2	0.67	3.85×10^{1}	3.85×10^{1}	10	1.90×10^{-2}	1.03×10^{-2}	5.19×10^{-17}	13.67	2.43×10^{-2}	3.55×10^{-4}	6.53×10^{-16}	3.43
NM1	3	0.60	2.65×10^{1}	2.65×10^{1}	6	3.94×10^{-3}	2.12×10^{-3}	9.39×10^{-18}	17.01	6.22×10^{-3}	9.08×10^{-5}	1.64×10^{-16}	2.94
NM1	4	0.49	1.45×10^{1}	1.45×10^{1}	3	3.36×10^{-4}	1.81×10^{-4}	6.86×10^{-19}	22.45	6.70×10^{-4}	9.78×10^{-6}	1.73×10^{-17}	2.47
NM1	5	0.32	2.5×10^{0}	2.5×10^{0}	0	4.17×10^{-6}	2.25×10^{-6}	7.09×10^{-21}	32.95	1.05×10^{-5}	1.53×10^{-7}	2.66×10^{-19}	1.52
NM2	1	0.58	6.25×10^{1}	6.25×10^{1}	12	1.41×10^{-2}	7.62×10^{-3}	3.11×10^{-17}	12.46	8.16×10^{-3}	1.19×10^{-4}	2.27×10^{-16}	3.69
NM2	2	0.50	3.85×10^{1}	3.85×10^{1}	9	3.13×10^{-3}	1.69×10^{-3}	6.65×10^{-18}	15.34	2.63×10^{-3}	3.85×10^{-5}	7.07×10^{-17}	3.60
NM2	3	0.45	2.65×10^{1}	2.65×10^{1}	6	1.31×10^{-3}	7.09×10^{-4}	2.74×10^{-18}	17.51	1.50×10^{-3}	2.19×10^{-5}	3.96×10^{-17}	3.12
NM2	4	0.37	1.45×10^{1}	1.45×10^{1}	3	3.16×10^{-4}	1.71×10^{-4}	6.46×10^{-19}	20.76	5.06×10^{-4}	7.39×10^{-6}	1.30×10^{-17}	2.50
NM2	5	0.25	2.5×10^{0}	2.5×10^{0}	0	2.39×10^{-5}	1.29×10^{-5}	4.79×10^{-20}	26.54	5.96×10^{-5}	8.71×10^{-7}	1.51×10^{-18}	1.60

Fig. S2: Vertical tortuosity increases as porosity declines during compaction (τ_v) (a) in kaolinite, smectite and intermediate mudstone models (b) in heterogenous mudstone models, *NM1* (designed after sample 1324C-1H-1) and *NM2* (designed after sample 1324B-7H-7).

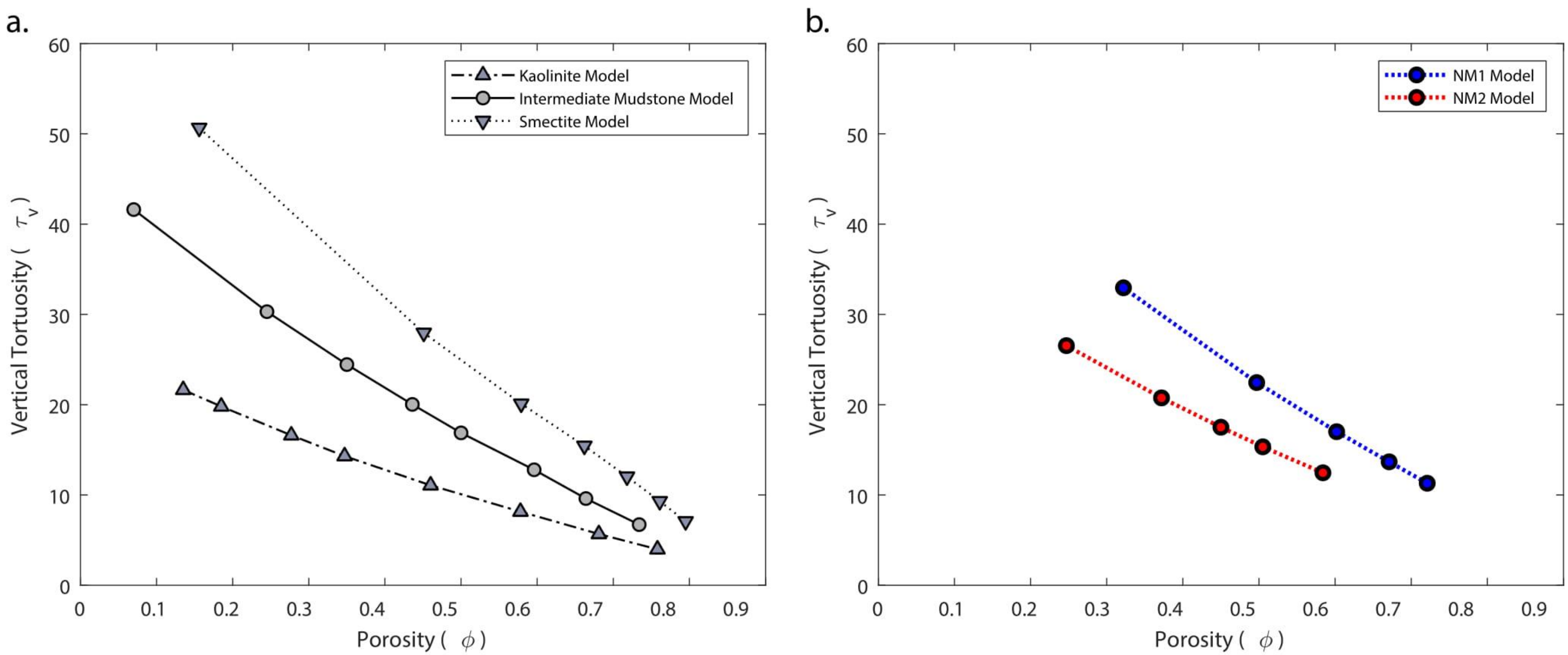

Table S3: Vertical flux (q_v^{mf}) during growth of microfractures through compacted intermediate mudstone, simulated by step-wise increase in microfracture width (ξ^{mf}).

Step	***Porosity*** ϕ	**Micro-fracture Width** ξ^{mf}	**Effective Fracture Width** ε_{eff}^{mf}	**Interbed Pore Throat Width** λ	**Vertical Flux** q_v^{mf}	**Reynolds Number Vertical flow** Re_v	**Vertical Permeability** k_v^{mf}
		(nm)	(nm)	(nm)	(m/s)		(m^2)
1	0.07	11.42×10^{0}	0.00×10^{0}	11.42×10^{0}	5.54×10^{-6}	1.24×10^{-5}	1.02×10^{-20}
2	0.10	57.14×10^{0}	1.37×10^{2}	11.42×10^{0}	1.56×10^{-4}	3.52×10^{-4}	2.89×10^{-19}
3	0.13	10.20×10^{1}	2.74×10^{2}	11.42×10^{0}	1.05×10^{-3}	2.37×10^{-3}	1.95×10^{-18}
4	0.18	18.28×10^{1}	5.14×10^{2}	11.42×10^{0}	7.99×10^{-3}	1.79×10^{-2}	1.48×10^{-17}
5	0.25	29.71×10^{1}	8.57×10^{2}	11.42×10^{0}	4.68×10^{-2}	1.05×10^{-1}	8.66×10^{-17}
6	0.29	37.70×10^{1}	1.10×10^{3}	11.42×10^{0}	1.12×10^{-4}	2.52×10^{-1}	2.07×10^{-16}

Table S4: Vertical flux (q_v^{frac}) during propagation of macrofracture through compacted intermediate mudstone, simulated by step-wise increase in fracture width (ξ^{frac}).

Step	***Porosity*** ϕ	**Macro-fracture Width** ξ^{frac}	**Effective Fracture Width** ε_{eff}^{frac}	**Interbed Pore Throat Width** λ	**Vertical Flux** q_v^{frac}	**Reynolds Number Vertical flow** Re_v	**Vertical Permeability** k_v^{frac}
		(nm)	(nm)	(nm)	(m/s)		(m^2)
1	0.07	11.42×10^{0}	0.00×10^{0}	11.42×10^{0}	5.54×10^{-6}	1.24×10^{-5}	1.02×10^{-20}
2	0.12	37.71×10^{1}	3.66×10^{2}	11.42×10^{0}	9.41×10^{-6}	2.11×10^{-5}	1.74×10^{-20}
3	0.17	70.85×10^{1}	6.97×10^{2}	11.42×10^{0}	1.17×10^{-5}	2.64×10^{-5}	2.17×10^{-20}
4	0.21	11.09×10^{2}	1.10×10^{3}	11.42×10^{0}	3.83×10^{-4}	8.60×10^{-4}	7.07×10^{-19}
5	0.25	14.74×10^{2}	1.46×10^{3}	11.42×10^{0}	5.81×10^{-3}	1.31×10^{-2}	1.07×10^{-17}
6	0.32	22.06×10^{2}	2.19×10^{3}	11.42×10^{0}	6.64×10^{-2}	1.49×10^{-1}	1.22×10^{-16}